IOPscience iopscience.iop.org

Home Search Collections Journals About Contact us My IOPscience

Calculation of prompt loss and toroidal field ripple loss under neutral beam injection on EAST

This content has been downloaded from IOPscience. Please scroll down to see the full text.

2017 Plasma Phys. Control. Fusion 59 025004

(http://iopscience.iop.org/0741-3335/59/2/025004)

View the table of contents for this issue, or go to the journal homepage for more

Download details:

IP Address: 134.148.10.13
This content was downloaded on 12/04/2017 at 04:08

Please note that terms and conditions apply.

You may also be interested in:

Energetic particles in spherical tokamak plasmas
K G McClements and E D Fredrickson

Collisional stochastic ripple diffusion of alpha particles and beam ions on TFTR
M.H. Redi, M.C. Zarnstorff, R.B. White et al.

Energetic particle physics in fusion research in preparation for burning plasma experiments
N.N. Gorelenkov, S.D. Pinches and K. Toi

Full particle orbit tracing with the RIO code in the presence of broad-spectrum MHD activity in a reversed-field pinch
J.A. Reusch, J.K. Anderson and Y. Tsidulko

Fast ion losses due to toroidal field ripple in JT-60U
K. Tobita, K. Tani, T. Nishitani et al.

Prompt non-resonant neutral beam-ion loss induced by Alfvén eigenmodes in the DIII-D tokamak
X. Chen, W.W. Heidbrink, G.J. Kramer et al.

The behaviour of fast ions in tokamak experiments
W.W. Heidbrink and G.J. Sadler

Fast ion ripple losses during neutral injection in TFR
M. Tuszewski and J.P. Roubin

Effect of fast-ion losses on plasma rotation
M. Honda, T. Takizuka, A. Fukuyama et al.

IOP Publishing Plasma Physics and Controlled Fusion
Plasma Phys. Control. Fusion 59 (2017) 025004 (11pp) doi:10.1088/1361-6587/59/2/025004

Calculation of prompt loss and toroidal field ripple loss under neutral beam injection on EAST

Bin Wu[1], Baolong Hao[1,2,3], Roscoe White[3], Jinfang Wang[1], Qing Zang[1], Xiaofeng Han[1] and Chundong Hu[1,2]

[1] Institute of Plasma Physics, Chinese Academy of Sciences, Hefei 230031, People's Republic of China
[2] University of Science and Technology of China, Hefei 230026, People's Republic of China
[3] Princeton Plasma Physics Laboratory, Princeton University, Princeton, NJ 08543, USA

E-mail: blhao@ipp.ac.cn

Received 26 September 2016, revised 20 October 2016
Accepted for publication 2 November 2016
Published 9 December 2016

Abstract

Neutral beam injection is a major auxiliary heating method in the EAST experimental campaign. This paper gives detailed calculations of beam loss with different plasma equilibria using the guiding center code ORBIT and NUBEAM/TRANSP. Increasing plasma current can dramatically lower the beam ion prompt loss and ripple loss. Countercurrent beam injection gives a much larger prompt loss fraction than co-injection, and ripple-induced collisionless stochastic diffusion is the dominant loss channel.

Keywords: neutral beam heating, toroidal field ripple, fast ion loss

(Some figures may appear in colour only in the online journal)

1. Introduction

The realization of magnetic confinement fusion energy requires a specially designed magnetic field configuration to prevent high-energy plasma particle loss from the confinement region for a sufficiently long time. Neutral beam injection (NBI) is a primary auxiliary heating method on tokamaks and other magnetic confinement facilities. The retention of beam-injected fast ions is a key issue for tokamak experiments [1]. EAST (Experimental Advanced Superconducting Tokamak) has developed two on-axis beam systems, one co-current beamline with an angle of 19.5° to the normal and another countercurrent beamline 17° to the normal; each beamline consists of two ion sources differing by 8.7°, which can be operated as two independent injectors. A superconducting tokamak has accessibility constraints due to limited port space, and tangentially injected beams have more ability to heat plasma and drive toroidal current. After a systematic study, the design is an excellent compromise between engineering constraints and heating efficiency. Figure 1 shows the layout of beamlines on EAST and the injection angles. The beamline at port A injects in the same direction as the plasma current, and the counter-injection beam system is connected to the F port of the facility [2]. This near-perpendicular injection geometry poses a threat to long pulse operation of EAST, because a hot spot due to fast ion loss on plasma-facing components may cause plasma disruption. The past several year's experiments obtained excellent neutral beam heating, with observed diagnostic measurement of fast ion loss using a fast ion loss detector and neutron measurement which have been developing on EAST, though the quantitative comparison between measurements and numerical calculation needs further investigation [3].

In the present EAST-NBI layout, the effective beam penetration can deliver fast ions to the center of the plasma, forming a steep fast ion density profile. In experiments performed over the last several years, the beam energy has been 35–65 keV and the gyro radius of beam ions ρ_L has been about 10^{-2} m, which means turbulence has no influence on the beam ion confinement. Considering magnetohydrodynamics (MHD)—quiescent plasmas—plasmas, the main loss mechanisms are first orbit loss and toroidal field ripple loss [4].

 © 2016 IOP Publishing Ltd Printed in the UK

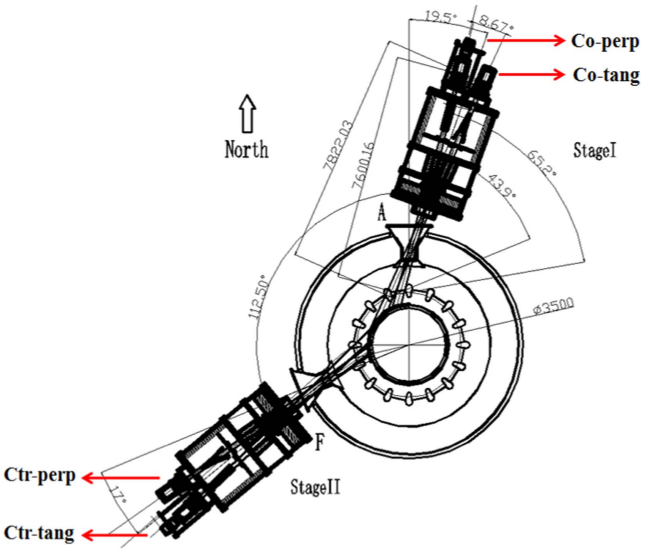

Figure 1. Schematic of the EAST neutral beam injection system.

In order to provide reference to the plasma physics experiment on EAST, in the following we first give quantified analysis of orbit loss and ripple loss using the guiding center code ORBIT and the NUBEAM module [5–7]. The initial beam ion distribution and steady-state deposition are obtained from a NUBEAM/TRANSP calculation [8]. All the analyses assume four independent beam injectors. The primary discharge analyzed is shot 61535, whose basic plasma parameters are shown in section 2. In section 3, beam ion prompt loss is discussed based on the initial beam ion distribution and different equilibria. Section 4 analyzes ripple loss using the EAST field ripple and also includes loss fraction dependence on plasma current. The magnetic geometry is generated using an EFIT equilibrium plus an analytically generated ripple field. The last section consists of discussion and conclusions.

Table 1. Plasma parameters for EAST discharge 61535.

Plasma current	$I_p = 440$ kA (counterclockwise)
Toroidal magnetic field on plasma center	$B_T = -2.2$ T (clockwise)
Major and minor plasma radius	$R_0 = 1.85$ m, a = 0.45 m
Elongation ration	$\kappa = 1.66$
Plasma shape	USN
Beam power injected	$P_{inj} = 0.9$ MW
Beam energy	$E_{nb} = 50$ keV

2. Calculation requirement

The beam ion distribution in the following calculation is generated by the NUBEAM module included in the TRANSP code. The input parameters for discharge 61535 at $t = 5.2$ s are shown in figure 2, and the plasma and beam parameters of this

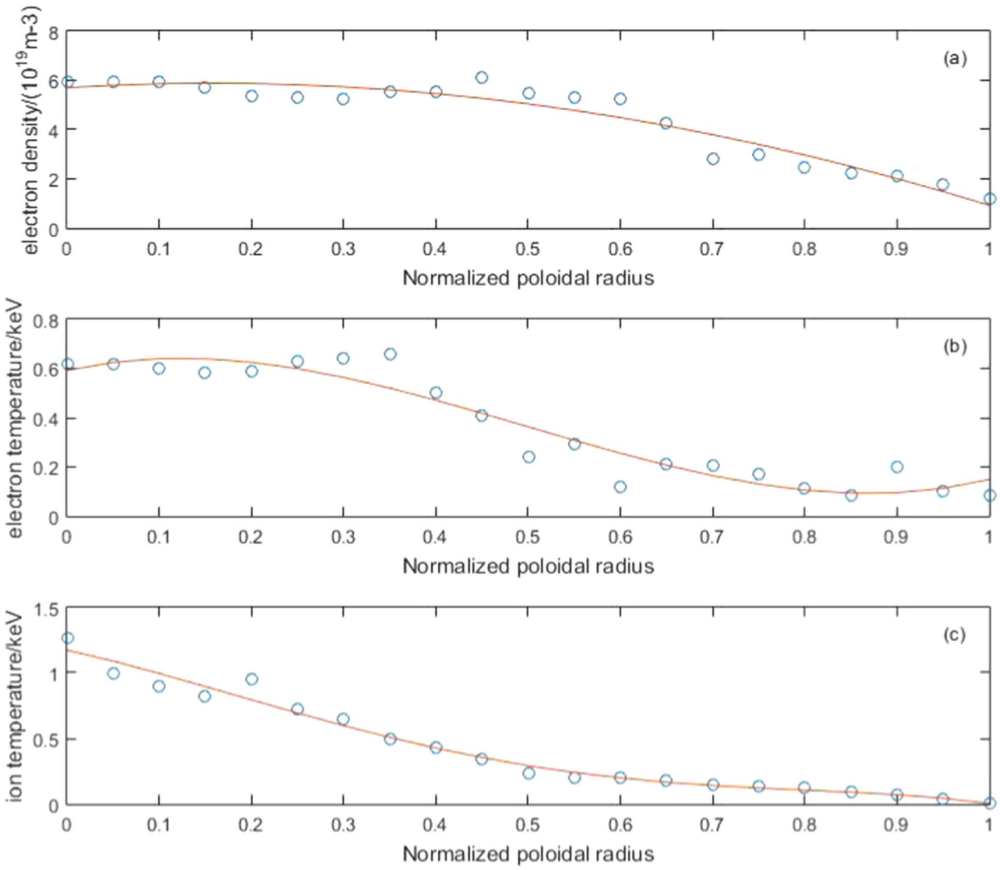

Figure 2. Plasma parameters of discharge 61535: (a) the electron density measured by Thomson scattering, (b) electron temperature measured by electron cyclotron emission, (c) ion temperature measured by CXRS (charge exchange recombination spectroscopy).

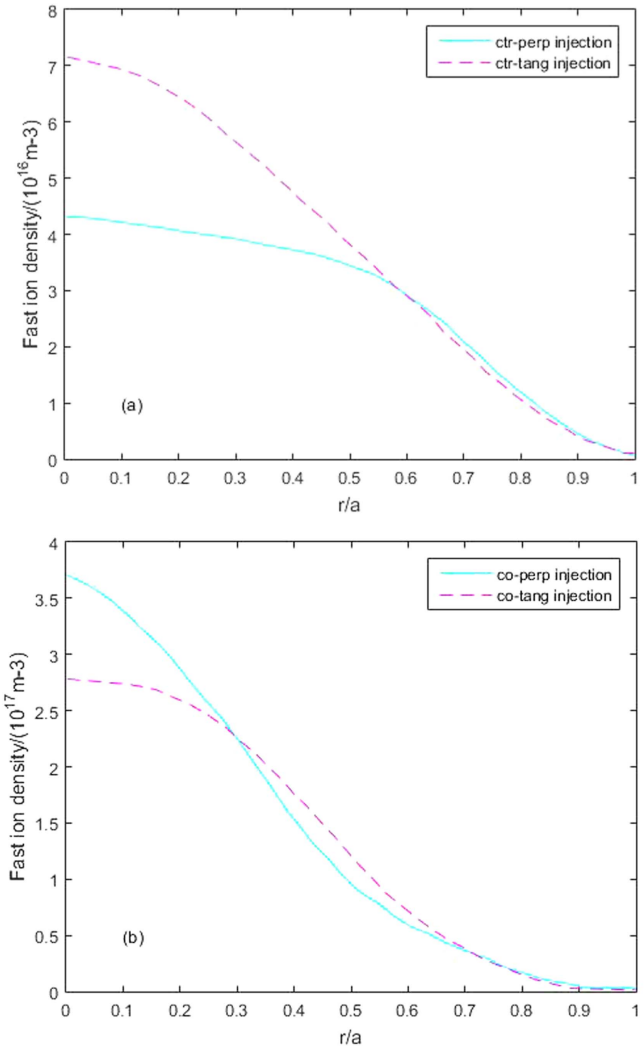

Figure 3. Beam ion, steady-state slowing down deposition profiles for four beam injectors: (a) countercurrent beam injection, (b) co-current beam injection.

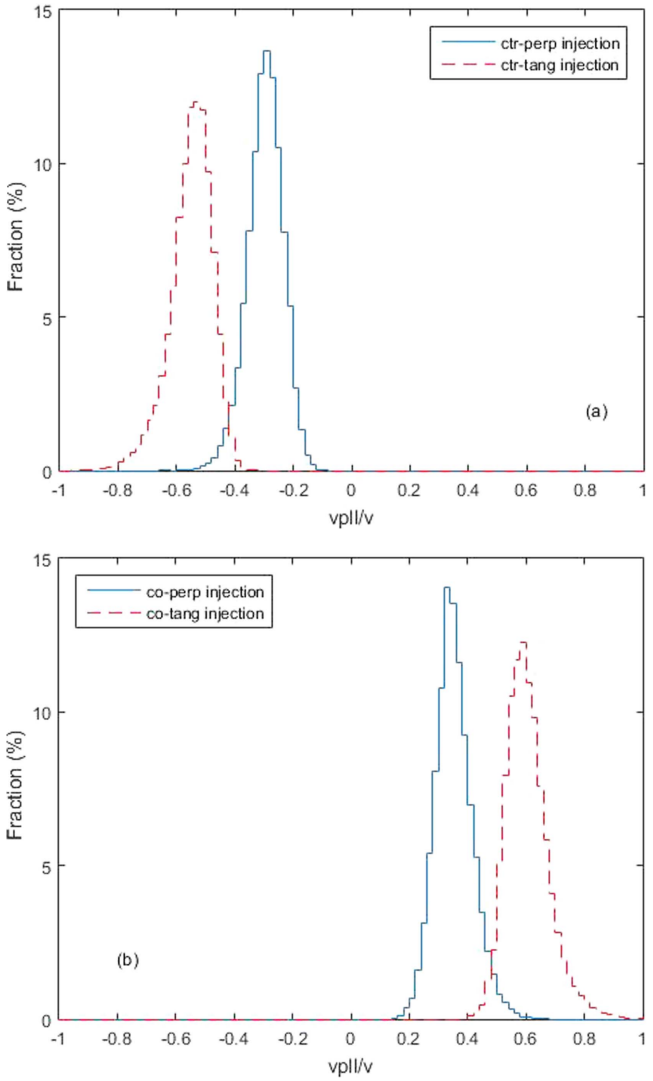

Figure 5. Pitch angle distribution fractions of initial beam deposition: (a) countercurrent beam injection, (b) co-current beam injection.

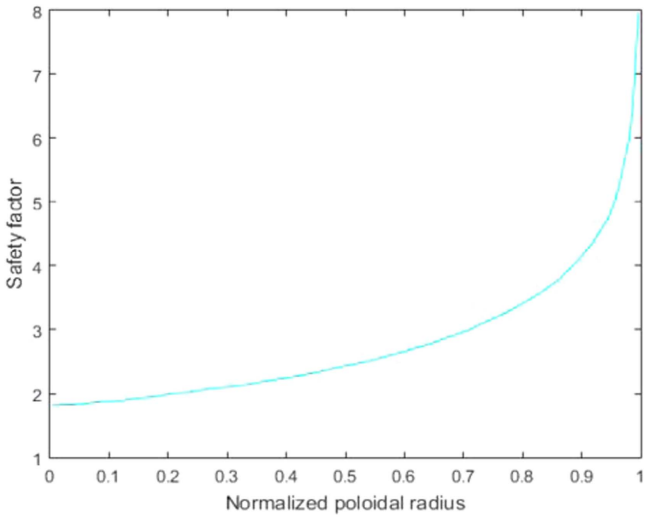

Figure 4. Safety factor profile of discharge 61535.

representative countercurrent beam heating plasma discharge are included in table 1. There are four neutral beam injectors on EAST, and the geometry of each injector is sketched in figure 1. The tangency radius of the co-tangent beam injector is 1.26 m, co-perp is 0.73 m, counter-perp is 0.61 m, and counter-tangent is 1.14 m. In shot 61535, the counter-tangent and counter-perp beam injectors each delivered 0.9 MW into the tokamak inner vessel. In order to compare the fast ion classical loss of each beam injector, each injector is considered alone with the same plasma background and beam parameters. The typical fraction of beam ions with full energy is about 80%; for beam energy of 50 keV and toroidal magnetic field of 2.2 T, the beam ion's transit time τ_{trans} is about 5.26 μs. The beam ion slowing down time is about 20 ms with $T_e(0) = 0.6$ keV, $ne(0) = 6 \times 10^{19}$ m^{-3}. During this slowing down time, fast ions should be confined well. Compared with higher plasma temperature and lower density discharge, shot 61535 has a shorter fast ion slowing down time.

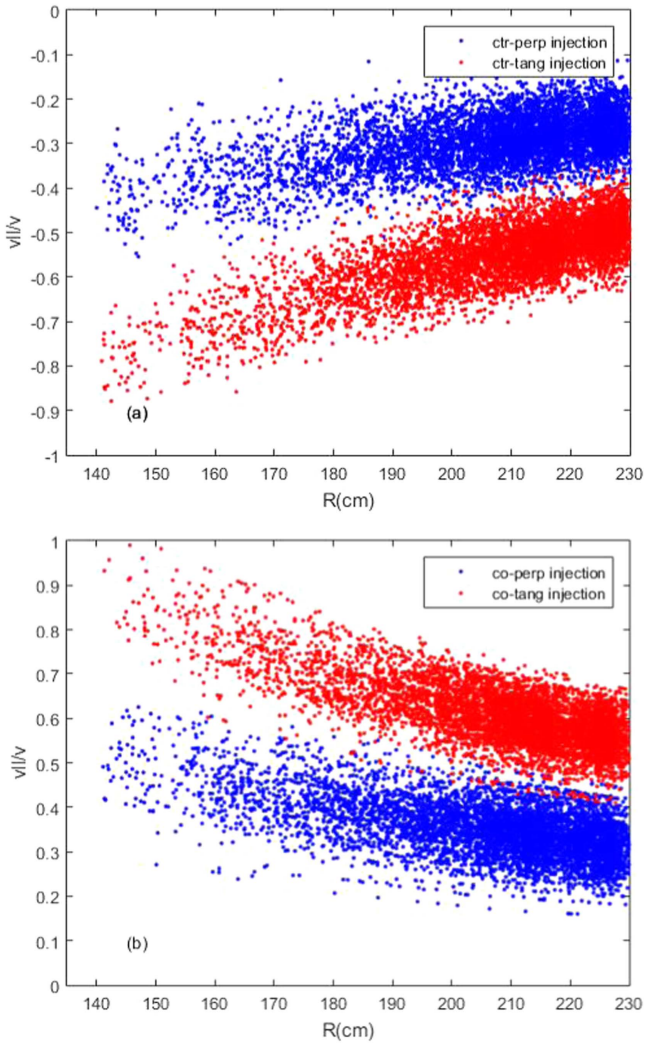

Figure 6. Initial beam ion pitch angle distributions as a function of major radius: (a) countercurrent beam injection, (b) co-current beam injection.

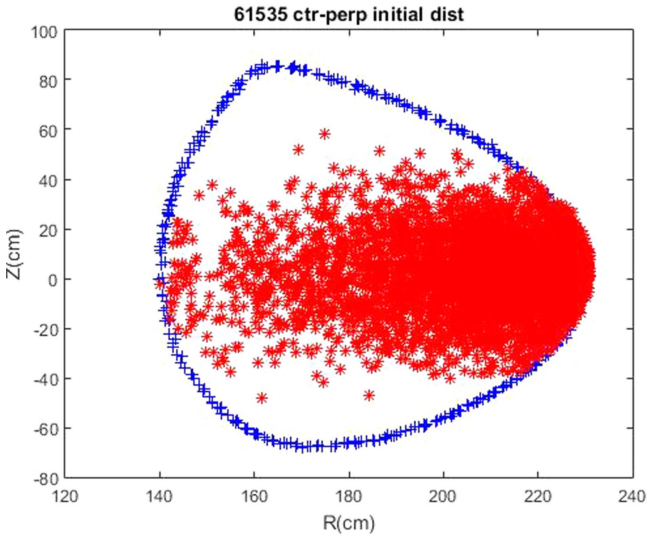

Figure 7. Spatial distribution of initial beam ion deposition in poloidal cross section for ctr-perp beam injection. Other injections have similar distribution, last closed flux surface shown as blue points.

Table 2. Calculation of beam ion prompt loss for shot 61535.

Neutral Beam Injector	Prompt Loss Fraction (%)
Co-tang	3.1
Co-perp	3.6
Ctr-tang	52.5
Ctr-perp	69.4

In general, higher electron density produces higher collisional drag and confines fast ions closer to the original flux surface; additionally, a lower fast ion slowing down time can reduce the particle loss time. But in the beam-heated plasma, higher electron density should be avoided at the edge region because fast ions generated at the plasma edge have more chance of loss to the first wall. Consequently, an optimized plasma density for beam ion confinement should be conducted with experimental scenarios scanning plasma parameters; this calculation only investigates changes in plasma current with a fixed beam ion distribution.

For given beam energy and injection geometry, the beam deposition profile is mainly determined by the electron density distribution provided there is no significant mode-particle resonance. Figure 3 shows the steady-state, slowing down beam ion density distribution profile of each beam injector calculated for shot 61535 as a function of normalized minor radius. The retention of fast ions under co-current beam injection is higher than countercurrent injection by an order of magnitude. With counter beam injection, the fast ion density with a near tangential injection angle is higher and more peaked than that with near perpendicular injection, which means better confinement. Near perpendicular injection of the co-current beamline has a higher peaked fast ion density in the core region compared with the co-tang injection, due to better beam penetration. These fast ion distributions can be used to assess neutral beam heating effect and analyze fast ion confinement.

All the calculations start from a particular beam ion distribution, assumed to be a plasma steady-state equilibrium. These equilibria are obtained from equilibrium reconstruction code EFIT, which was applied in the EAST experiment for plasma shape control and physical analysis [9]. Monotonic sheer q profiles are maintained when the plasma current is modified. The safety factor profile of shot 61535 is shown in figure 4, and the boundary safety factor q_{95} is about 5.

3. Prompt loss

Beam ion confinement mainly depends on the fast ion distribution and magnetic configuration. After ionization, assuming axisymmetry, particle orbits are closed, with functions only of the magnetic moment, energy, and canonical momentum. If an orbit intersects the wall or divertor within the first poloidal orbit, this leads to prompt loss. The orbit

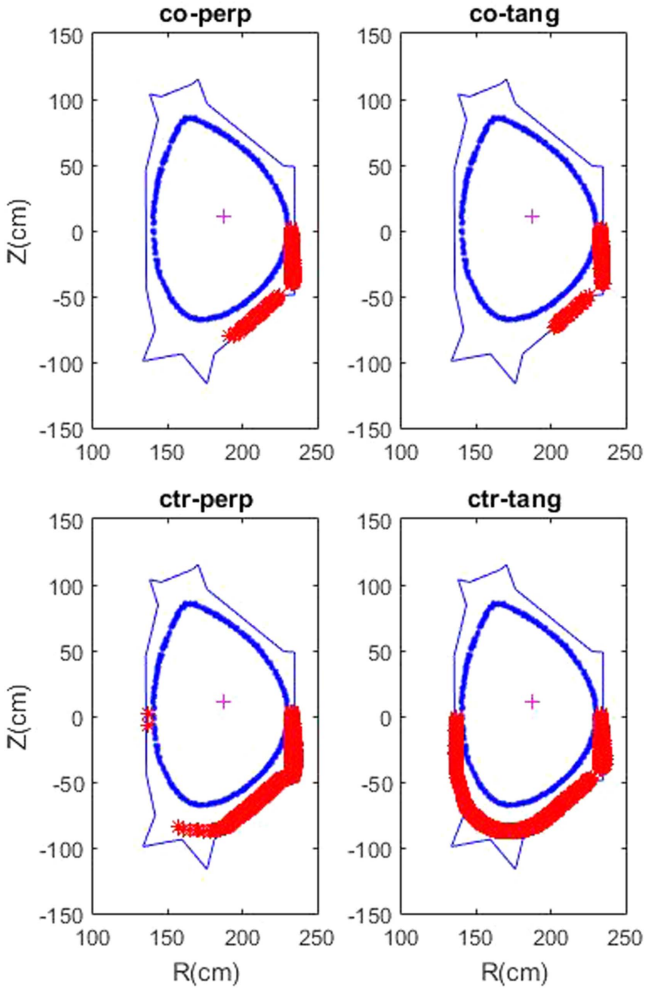

Figure 8. Poloidal location of striking point on the nominal flux surface outside of the plasma edge for beam ion prompt loss calculation, carried out by the NUBEAM module.

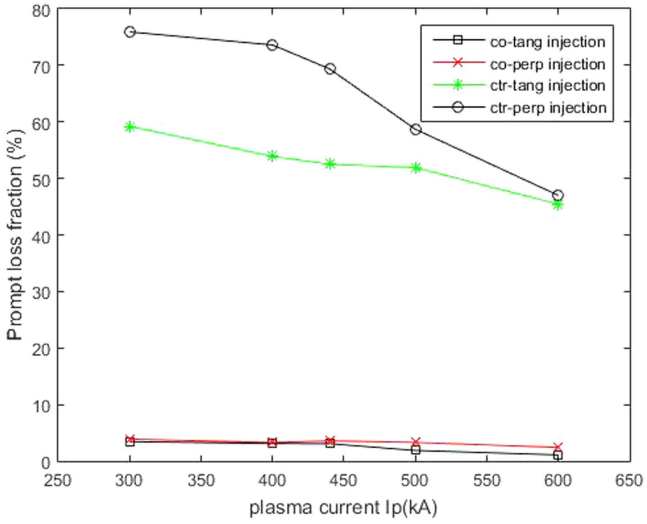

Figure 9. Prompt loss fraction of four beam injectors versus plasma current.

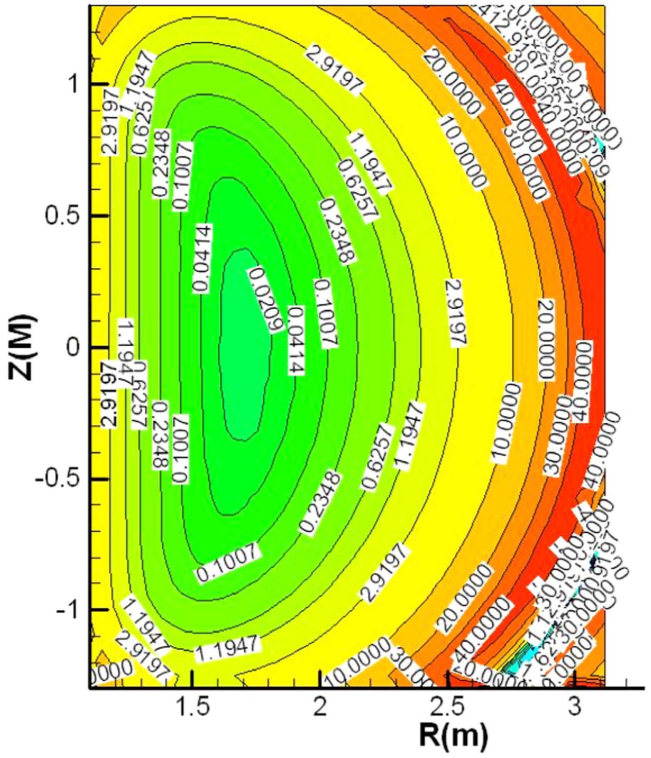

Figure 10. Toroidal field ripple δ using percent contour in the cross sectional view of toroidal coils on EAST.

width of a passing particle is about $q\rho_L$, with q the safety factor. For typical equilibria on EAST, q is about 2–3, so the radial excursion from the initial flux surface for a far-passing beam ion can't lead to significant prompt loss. For the banana-trapped fast ions, this excursion is about $2\sqrt{2R/r}\,q\rho_L$, that is, about 20–30 ρ_L on EAST, and this orbit width is comparable to the minor radius of the machine and can produce significant beam ion prompt loss [10].

To be trapped between turning points by magnetic mirrors on the outside of the torus, the fast ion's pitch angle $\alpha\left(\sin\alpha \equiv \frac{v_\perp}{v}\right)$ at the poloidal outside (poloidal angle $\theta \approx 0$) must satisfy $\sin\alpha \geqslant \sqrt{B_{\min}/B_{\max}} \equiv \sqrt{R_0 - r/R_0 + r}$, defining a loss-cone boundary at the weaker field side of the torus. The initial beam ion distribution as a function of $v_\parallel/v\,(=\cos\alpha)$ is shown in figure 5, and the pitch angle as a function of major radius is shown in figure 6. The beam ion pitch angle distribution for near-perpendicular injection is smaller than with tangential injection, so there are more beam ions within the loss-cone boundary. Also, the banana-trapped beam ion fraction is larger than with tangential injection. Plasma operation should avoid higher plasma density or density gradient near the edge region, preventing higher beam ion deposition as banana-trapped particles.

The penetration of neutral beams on EAST produces successful deposition at the plasma center; the initial spatial distribution of beam ions after ionization is shown in figure 7 for shot 61535. In the weaker field area near the outside of the

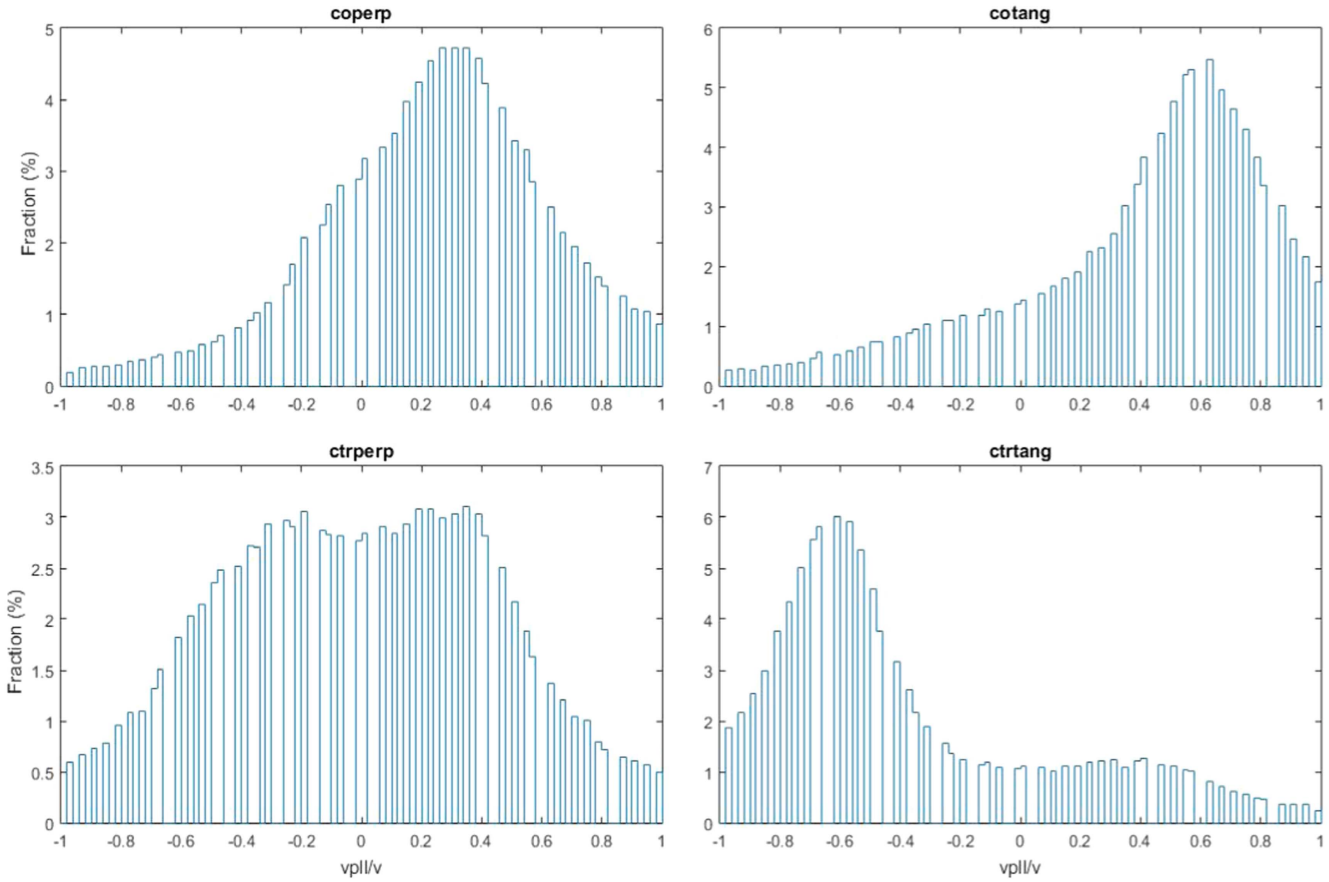

Figure 11. Calculated pitch angle distributions of steady-state, slowing down beam ions.

torus, co-injected beam ions drift inward after ionizing and their orbits remain inside the initial flux surface. Conversely, counter-injected beam ions launched from the weaker field side drift outward, causing more prompt loss. For the primary discharge investigated here, shot 61535, calculation results of prompt loss for the four beam injectors are presented in table 2.

These calculations indicate that the beam ion prompt loss of the countercurrent injection is much larger than with the co-current injection due to radial drift and larger banana-trapped fraction. The beam ion prompt loss distribution in the poloidal direction is shown in figure 8. The hot spot is just below the outer equatorial plane due to the downward gradient B drift on the outer part of the banana orbit. In case of co-injection, beam ions on the upper part of the orbit always move inward as the poloidal projection of banana orbits move radial outwards and escape below the midplane eventually; the counter-injected beam ions escape from below the midplane.

Since the orbit width is proportional to qr_L, the gyro radius in the poloidal magnetic field, the simplest way to reduce orbit width is to raise the plasma current. To compare the influence of plasma current on the beam ion prompt loss, we simulated several cases with a range of plasma current from 300 to 600 kA, all equilibria with similar toroidal field and q shapes. Figure 9 presents these simulation results; the plasma current dependence of prompt loss reveals that increasing plasma current can reduce the orbit width effectively and the loss fraction decreases dramatically, especially for the counter-injected beam ions. There is little prompt beam ion loss for co-current injection but significant loss for countercurrent injection because of the larger orbit width and outward radial drift direction.

4. Toroidal field ripple loss

The timescale of beam ion prompt loss is less than 10^{-4} s, which is much shorter than the collision time. Coulomb collisions and toroidal ripple perturbation have very little influence on the beam ion prompt loss. Toroidal field ripple originates from the inherent discrete nature of toroidal coils; this periodic perturbation amplitude can be defined as $\delta(r, \theta) = (B_{\max} - B_{\min})/(B_{\max} + B_{\min})$. There are 16 coils on EAST and the magnetic geometry of the tokamak can be expressed by $B = B_0(1 - \varepsilon\cos\theta)(1 - \delta(r, \theta)\cos N\phi)$, where $N = 16$ and $\varepsilon = r/R$. The magnetic field near the toroidal coils is stronger than between the coils; this variation of magnetic field along a field line can act like a magnetic mirror, and the criterion to form a secondary magnetic well in the circular cross section tokamak is $\alpha(r, \theta) = \varepsilon|\sin\theta|/Nq\delta \leqslant 1$. Beam ions with small enough parallel velocity can be trapped toroidally in this ripple well when $|v_\parallel/v| \leqslant \sqrt{\delta}$. Locally ripple-trapped fast ions execute

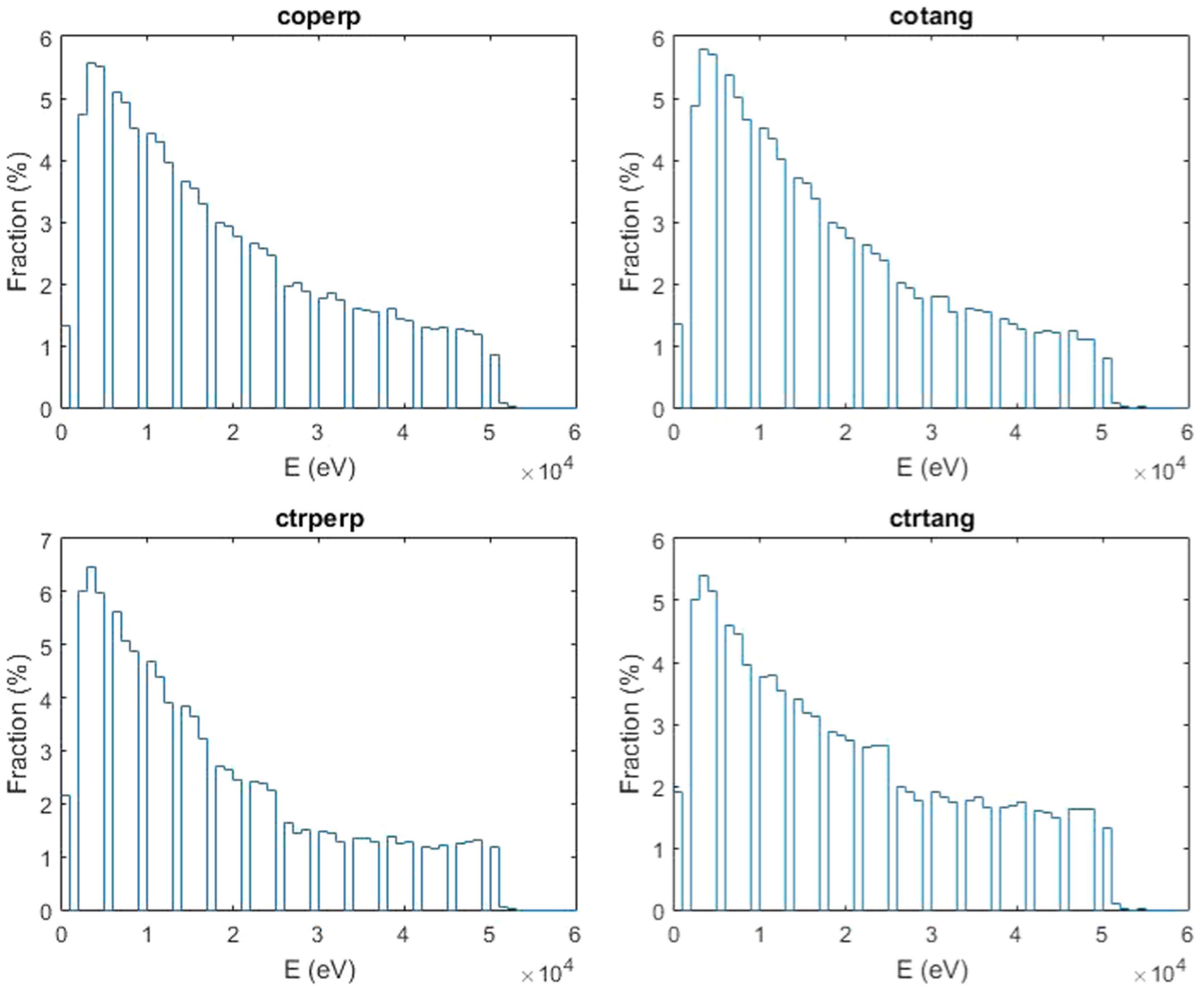

Figure 12. Energy distribution of beam ions with steady-state deposition.

Table 3. Calculation of beam ion ripple loss for shot 61535.

Neutral Beam Injector	Ripple Loss Fraction (%)
Co-tang	5.1
Co-perp	16.9
Ctr-tang	18.7
Ctr-perp	35.9

superbanana orbits and drift vertically in the gradient B direction until they escape from the plasma or are kicked out of the ripple well by collisional scattering. On current tokamaks, this ripple well region only exists over a minor area on the outer side of plasma near the equatorial plane. The EAST ripple amplitude δ is about 0.6% at the outer plasma boundary on the equatorial plane, about 0.2% at the inner plasma boundary, and less than 0.02% at the near plasma core; the distribution of ripple is shown in figure 10. To be ripple well trapped on EAST, the beam ion's pitch angle at the outer edge region should be $|v_{\|}/v| \leqslant 0.07$, which is a very minor proportion of the steady-state, slowing down beam ion pitch angle distribution, as shown in figure 11. Because the fast ion density at the plasma periphery is very low, as shown in figures 3 and 4, few beam ions can be lost through ripple well trapping directly.

Broken axisymmetry due to discrete toroidal coils not only brings about the presence of the local magnetic ripple well, but produces radial displacement near the banana particle's bounce point. The radial position modification of a banana tip after one poloidal transit is about $\Delta r \simeq (N\pi/|\sin\theta_b|)^{\frac{1}{2}}\,(q/\varepsilon)^{\frac{3}{2}}\rho_L\delta\,\cos(N\Delta\phi_b)$, where θ_b is the poloidal angle of the bounce point and $\Delta\phi_b$ is the toroidal angle difference of consecutive bounce points. The radial displacement in the vicinity of the turning point leads to failure of orbit closure, which can produce diffusive loss with sufficiently large amplitude or enough collisions. Collisions can produce stochastic diffusion if the fast ions have received enough collisional scattering within one bounce time to decouple consecutive banana orbits. The criterion of collisional frequency $\nu_{criterion}$ for beam ions entering into the ripple-

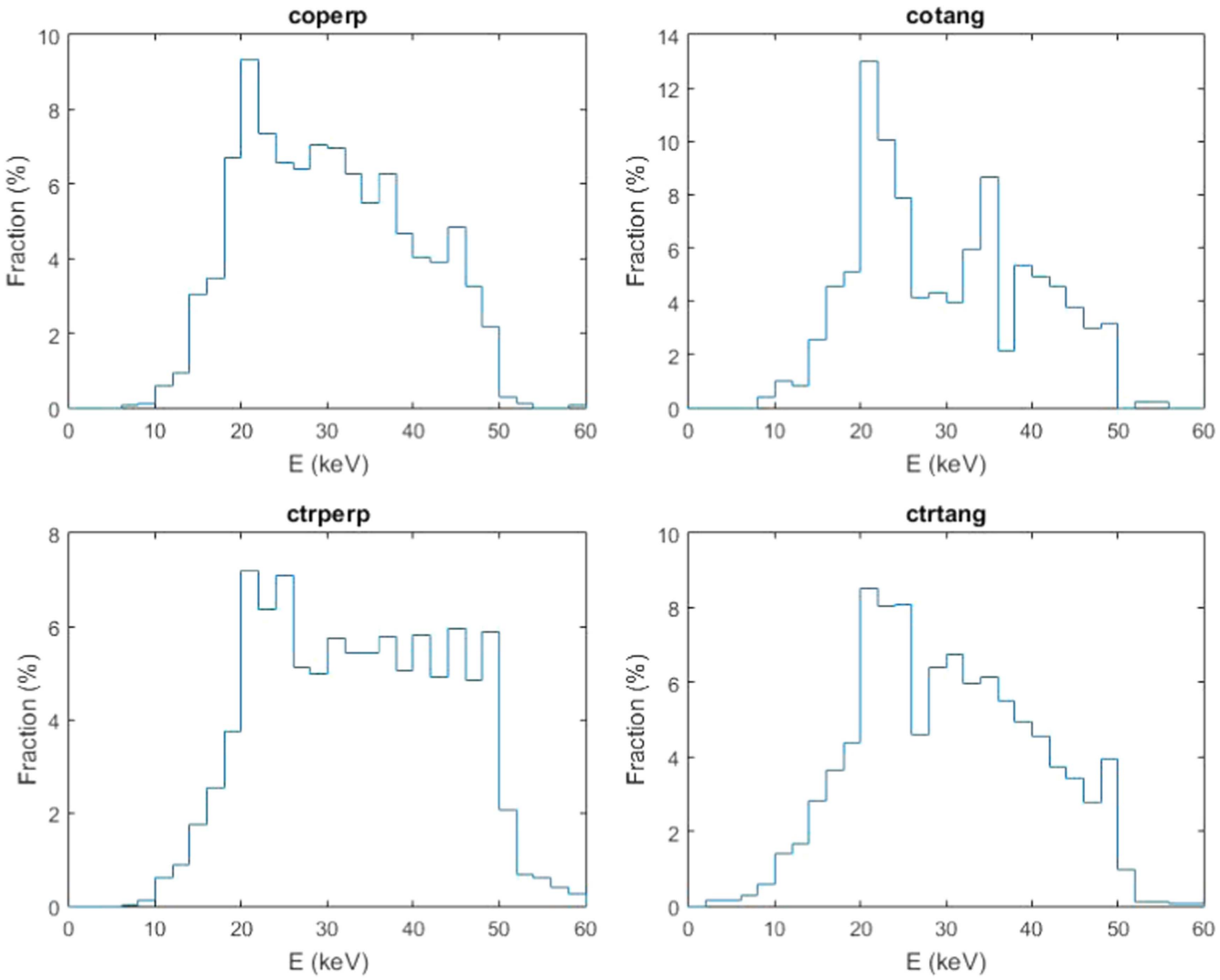

Figure 13. Energy distribution of lost particles from beam ion ripple loss calculation.

induced diffusive transport regime is $\nu^*/\nu_{criterion} < (Nq)^2$, with $\nu^* = \varepsilon\omega_b/2\pi$ [11, 12]. Pitch angle scattering for shot 61535 is about $\nu_{collision} \simeq 0.26\ s^{-1}$, bounce frequency ω_b is about $\omega_b \sim 10^5$ Hz, and the $\nu_{criterion}$ is about $\nu_{criterion} \sim (1-3)\ s^{-1}$, so the collisions are too weak to decouple turning point oscillations and give rise to stochastic ripple diffusion. An analytical approximation for ripple strength threshold for the onset of collisionless stochastic ripple diffusion in the vicinity of the banana tips is $\delta_s = [\varepsilon/N\pi q]^{3/2}/\rho_L q'$, with $q' = dq/dr$ [13]. This criterion specifies a collisionless banana drift diffusion domain which has a sensitive dependence on the safety factor profile or plasma current operation [14]. Shot 61535 has a plasma current of 440 kA, counterclockwise from above. The q profile and other plasma parameters are shown in figures 4 and 2. The equilibrium configuration in this paper is described by EFIT, with the EAST ripple distribution fitted with an analytic function $\delta(R, Z) = \delta_0 \exp\{[R - R_{rip})^2 + b_{rip}Z^2]^{1/2}/w_{rip}\}$ [6, 15–17], with coefficients $\delta_0 = 1.267 \times 10^{-4}$, $R_{rip} = 1.714 - 0.181Z^2$, $b_{rip} = 0.267$, $w_{rip} = 0.149$ m.

Ripple loss calculation begins with the steady-state, slowing down beam ion distribution. The energy distribution of shot 61535 is shown in figure 12. Other distribution information is presented in figures 3, 4, 11. All the calculations of the work followed specific distributions of 10 000 particles until they escaped from the last closed flux surface or up to half of the beam ion slowing down time, about 2000 toroidal transits. Collisional drag and scattering of beam ions is done with a Monte Carlo operator. Plasma parameters needed in calculating these collision rates are shown in figure 2. Table 3 shows the calculation results of beam ion ripple loss for the four independent beam injectors. Particle loss with near-perpendicular injection is greater than with tangential beam injection since the banana particle fraction for near-perpendicular injection is larger than for tangential injection and the ripple field only affects banana-trapped particles. Beam ion ripple loss with co-current injection is smaller than with countercurrent injection due to the radial drift direction after the beam ion is launched. Banana orbits of beam ions under counter-injection drift outwards and

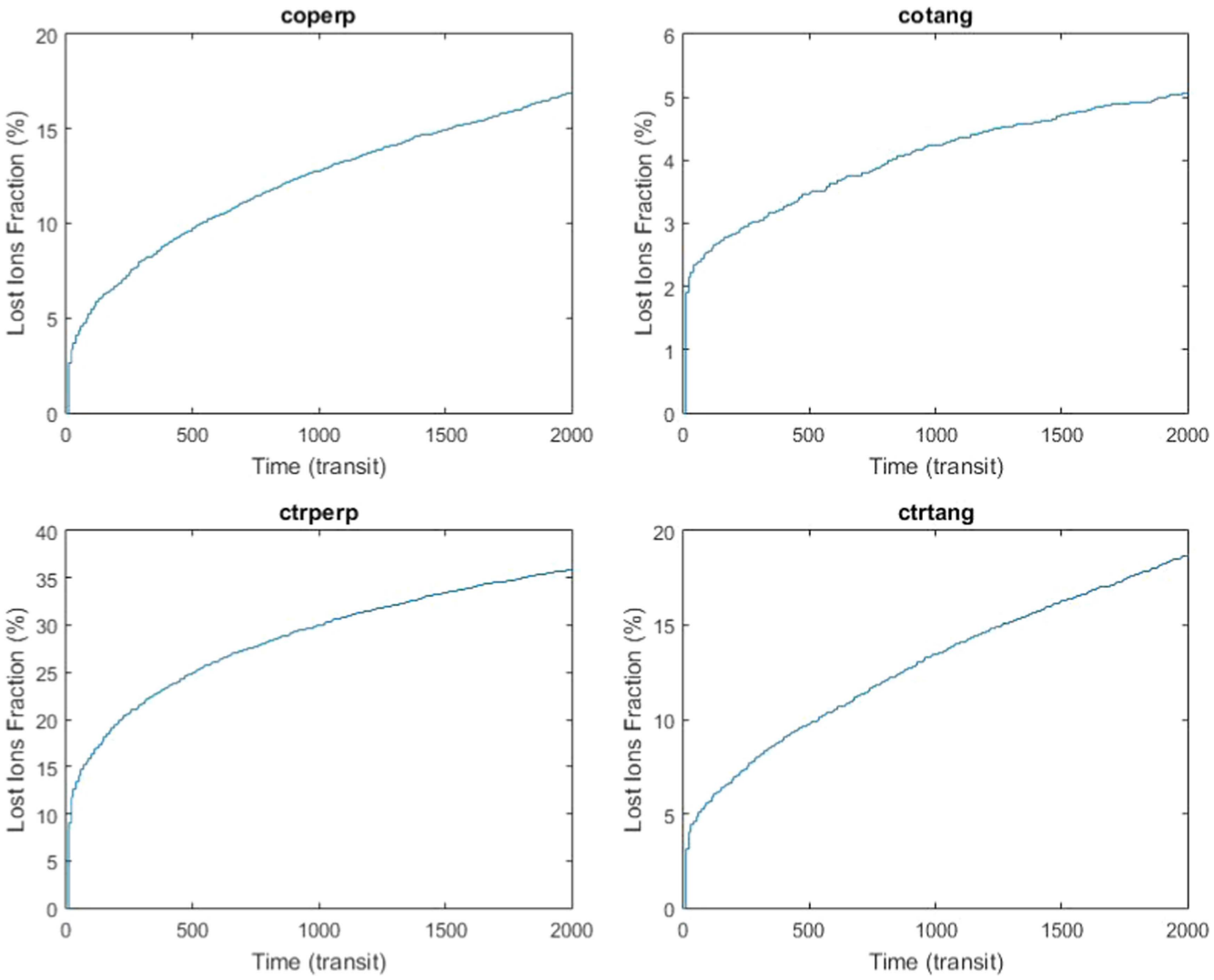

Figure 14. Beam ion ripple loss fraction evolved as a function of toroidal transits over half the slowing down time.

encounter greater ripple. The energy distribution of lost beam ions is shown in figure 13. Evolution of the particle loss fraction presented in figures 14, 15 shows that the ripple-induced particle loss occurred just below the outer midplane. The width of the poloidal distribution of lost particles increases with particle energy, and thus inversely with escape time. To consider orbits traversing the last closed flux surface, loss fraction and load pattern will be changed slightly due to ions reentering the plasma region, but we expect this calculation can give a good reference to experiment analysis on EAST.

Plasma current on EAST is presently in the range of 300–600 kA, and the ripple-induced beam ion stochastic diffusion is very sensitive to the current profile. This work calculated fast ion ripple loss for the four beam injectors with different plasma currents, from 300 to 600 kA, as shown in figure 16. Ripple loss of all beam injectors decreased when plasma current increased. For given plasma shape and toroidal field, increasing plasma current can lower the safety factor, which benefits the fast ion confinement in MHD-quiescent plasmas, provided one avoids the destabilization of the kink mode. Increasing plasma current can lower the fraction of banana particle chaotic orbits by decreasing the banana tip perturbation.

5. Conclusions

Using guiding center code ORBIT and NUBEAM/TRANSP, this paper performed a detailed calculation of the beam ion prompt loss and toroidal field ripple loss. Beam ion banana stochastic diffusion on EAST is the dominant ripple loss process, since the ripple amplitude in the plasma area is too small to produce ripple trapping. The calculation shows that the prompt loss and ripple loss can be lowered effectively by increasing the plasma current. Other methods to improve the beam heating include increasing the outer gap to move the plasma to a region of smaller ripple and optimizing the plasma density profile to lower fast ion density at the outer plasma edge.

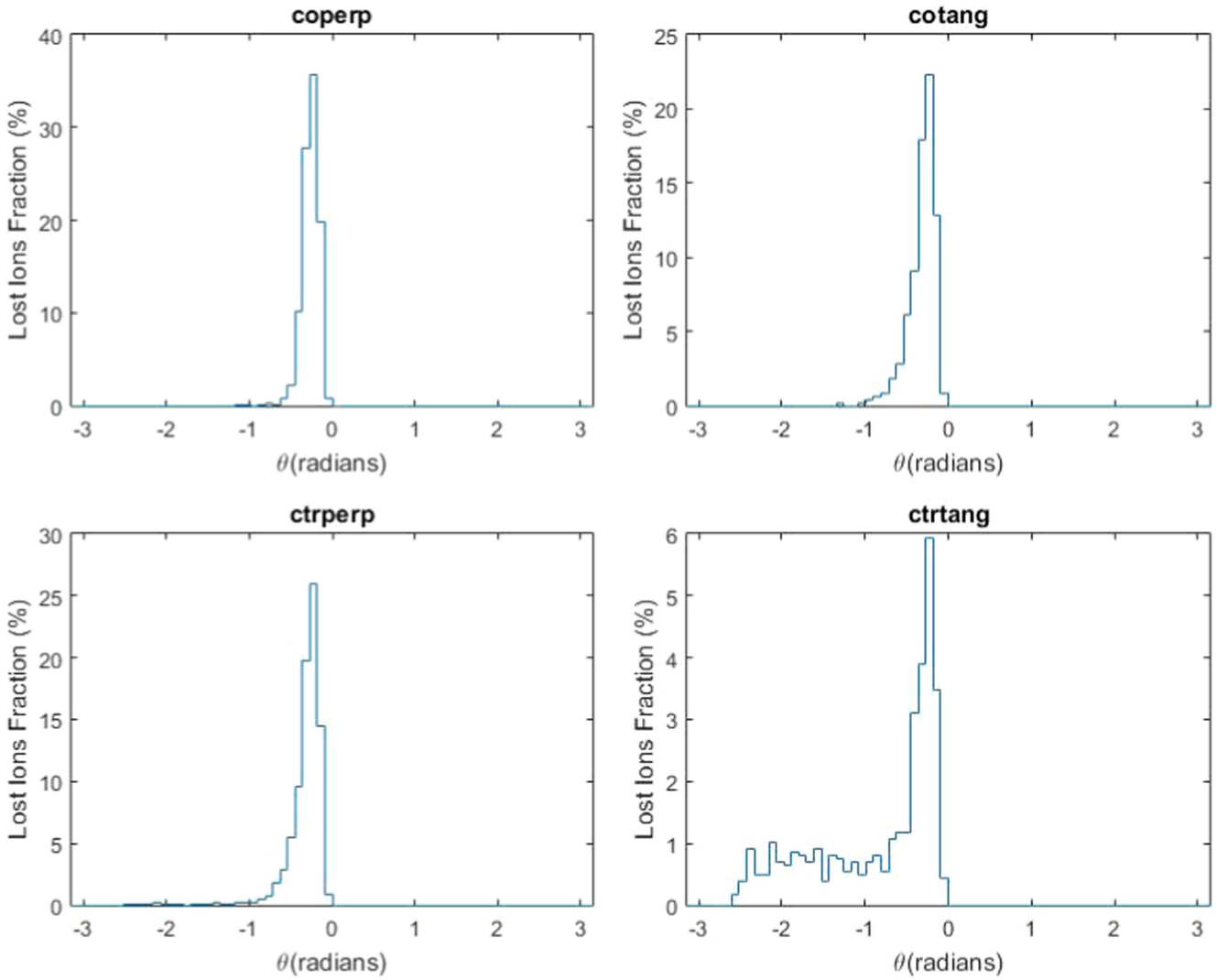

Figure 15. Lost particle poloidal angle distribution from beam ion ripple loss.

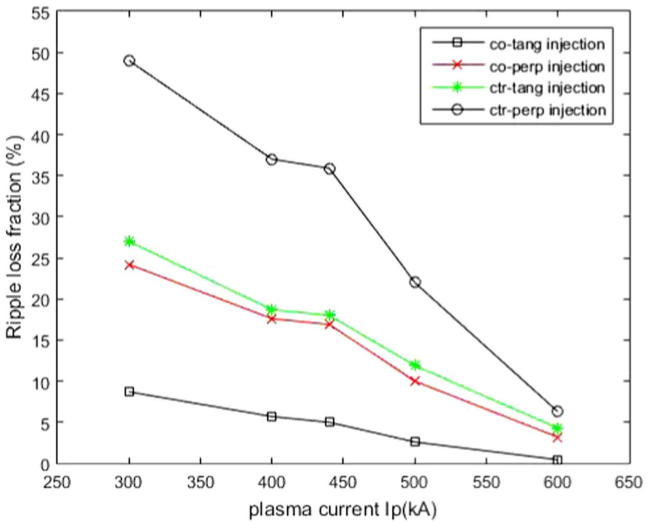

Figure 16. Plasma current dependence of beam ion ripple loss fraction with a current range.

Acknowledgments

The authors wish to thank M A Van Zeeland for help with NUBEAM and useful discussions, and are also grateful for the support of the EAST Contributors, especially Yuntao Song, Youjun Hu, Juan Huang, Guoqiang Li, Siye Ding, and Zhengping Luo. This work was supported by the National Magnetic Confinement Fusion Science Program of China (Contract No. 2013GB101001), the International Science & Technology Cooperation Program of China (Contract No. 2014DFG61950), and the National Natural Science Foundation of China (Contract Nos. 11628509 and 11405212).

References

[1] Wesson J 2011 *Tokamaks* 4th edn (New York: Oxford University Press) p 169

[2] Wang J F, Wu B and HU C D 2010 Simulation on heating and current drive using neutral beam injection with variable injection angle on EAST *Plasma Sci. Technol.* **12** 289
[3] Zhu Y B, Heidbrink W W and Pickering L D 2010 Phenomenology of energetic-ion loss from the DIII-D tokamak *Nucl. Fusion* **50** 084024
[4] Strumberger E *et al* 2008 Fast particle losses due to NTMs and magnetic field ripple *New J. Phys.* **10** 023017
[5] Gorelenkov N N and White R B 2013 Perturbative study of energetic particle redistribution by Alfvén eigenmodes in ITER *Plasma Phys. Control. Fusion* **55** 015007
[6] Redi M H, Zarnstorff M C and White R B 1995 Collisional stochastic ripple diffusion of alpha particles and beam ions on TFTR *Nucl. Fusion* **35** 1191
[7] White R B, Goldston R J and McGuire K 1983 Theory of mode induced beam particle loss in tokamaks *Phys. Fluids* **26** 2958–64
[8] Pankin A, McCune D and Andre R 2004 The tokamak Monte Carlo fast ion module NUBEAM in the national transport code collaboration library *Comput. Phys. Commun.* **159** 157–84
[9] Li G Q and Ren Q L 2013 Kinetic equilibrium reconstruction on EAST tokamak *Plasma Phys. Control. Fusion* **55** 125008
[10] Hynonen V *et al* 2008 Upgrade team effect of radial electric field and ripple on edge neutral beam ion distribution in ASDEX upgrade *Plasma Phys. Control. Fusion* **50** 035014
[11] Boozer A H 1980 Enhanced transport in tokamaks due to toroidal ripple *Phys. Fluids* **23** 2283–9
[12] Tobita K, Tani K and Nishitani T 1994 Fast ion losses due to toroidal field ripple in JT-60U *Nucl. Fusion* **34** 1097
[13] Goldston R J, White R B and Boozer A H 1981 Confinement of high energy trapped particles in Tokamaks *Phys. Rev. Lett.* **47** 647
[14] White R B 2014 The theory of toroidally confined plasmas 3rd edn (Singapore: World Scientific) p 63
[15] Redi M H *et al* 1996 Simulations of alpha particle ripple loss from the international thermonuclear experimental reactor *Phys. Plasmas* **3** 3037
[16] Boivin R L, Zweben S J and White R B 1993 Study of stochastic toroidal field ripple losses of charged fusion products at the midplane of TFTR *Nucl. Fusion* **33** 449–62
[17] Honda M, Takizuka T and Fukuyama A 2008 Numerical analysis of the effect of fast-ion losses on plasma rotation in a tokamak with toroidal field ripple *Nucl. Fusion* **48** 085003